

Astrometry24.NET – precise astrometry for SST and NEO

Agnieszka Sybilska^{a*}, Stanisław Kozłowski^b, Piotr Sybilski^a, Rafał Pawlaszek^a, Mariusz Slonina^a, Agnieszka Gurgul^a, Piotr Konorski^a, Michał Drzał^a, Sławomir Hus^a, Grzegorz Lech^a, Michał Litwicki^b, Maciej Pilichowski^a, Rafał Ślimak^a, Ulrich Kolb^c, Vadim Burwitz^d, Tim Flohrer^e, Quirin Funke^e

^a Sybilla Technologies, ul. Toruńska 59, 85-023 Bydgoszcz, Poland, agnieszka.sybilska@sybillatechnologies.com

^b Cilium Engineering, ul. Łokietka 5, 87-100, Toruń, Poland

^c School of Physical Sciences, The Open University, Walton Hall, Milton Keynes MK7 6AA, United Kingdom

^d Max-Planck-Institut für Extraterrestrische Physik, Giessenbachstrasse, 85748 Garching, Germany

^e ESA/ESOC Space Debris Office (OPS-GR), Robert-Bosch-Str. 5, 64293 Darmstadt, Germany

* Corresponding Author

ABSTRACT

Astrometry24.NET (A24N) is the first openly available online tool for precise astrometry of astronomical objects able to provide an astrometric solution for both point sources as well as streaks left by non-sidereal moving objects (satellites and space debris or Near-Earth Objects - NEOs).

A24N is accessible by the end user through three interfaces a) a web browser with modern, responsive UI, b) a cross-platform Command Line Interface (CLI) and c) programmatically through a RESTful API. It makes use of state-of-the-art IT technologies and specifically developed detection and analysis algorithms, utilizing cloud premises, which allow for inexpensive Service Level Agreement (SLA) up to 99.9%. Processing is available on-demand, with optimized load balancing, depending on the actual usage. The architecture of the system, catalogue support, and the astrometric engine behind A24N are first described, followed by the description of the dedicated web portal, built on top of Sybilla Technologies AstroDrive engine, which enables the user to easily upload, store, search, view and manipulate their data.

We show the results obtained by the service from synthetic and real data sets. NEO data from ESA Optical Ground Station (OGS) were used, reduced with A24N, Astrometrica and compared (as ground truth) with ephemerides provided from JPL Horizons. For the simulated data tests, a dedicated synthetic frames generator has been developed, which allows one to reproduce all major error sources and isolate their effect.

A24N has been tried and tested on a number of data sets from various observatories, including the ESA OGS and the Test Bed Telescope (TBT) in Spain, as well as observatories belonging to the Open University (UK), Nicolaus Copernicus Astronomical Center of the Polish Academy of Sciences (Poland), Max Planck Institute for Extraterrestrial Physics (Germany, COG), Mt. Suhora Observatory of the Pedagogical University in Cracow (Poland), and Comenius University (Slovakia).

Long-term monitoring of the COG sensor accuracy, precision and offset has been conducted, as well as observations of Geostationary Orbit (GEO) drifters to test the algorithms and architecture in the production environment. The results of the campaign are presented.

1 INTRODUCTION

The Earth orbit is becoming more and more populated by functioning satellites and space debris. The tracked and counted objects amount to ca. 15 000 as of 2017 (see, e.g. [1]) and these numbers only cover objects larger than 0.1m in the Low-Earth Orbit (LEO) and 0.3-1.0m in the Geostationary Orbit (GEO). It is estimated that as many as 750 000 objects larger than 1cm are orbiting the Earth.

The goals of the Space Surveillance and Tracking (SST) segment of the ESA Space Situational Awareness programme are the detection, identification, cataloguing and tracking of space debris and satellites. Up-to-date knowledge of the whereabouts of space objects is crucial to maintaining orbital safety and continued usability of the orbits. Also, collision mitigation helps extend lifetimes of active and functioning satellites.

Obtaining an accurate astrometric solution for a given frame or data set is a prerequisite to the subsequent calculation of exact coordinates and/or orbital parameters of tracked/discovered objects. A number of tools exist, ranging from free specialist, Linux-based tools requiring significant user and input data preparation (Astromatic software suite of [2] and later ones), through Windows-based commercial downloadable applications (PinPoint¹, Astrometrica²), to the online Astrometry.net of [3] requiring as little of the user as uploading the chosen image to their service. None of the tools is, however, suited for streak extraction as they only offer point-source recognition.

¹ <http://pinpoint.dc3.com/>

² <http://www.astrometrica.at/>

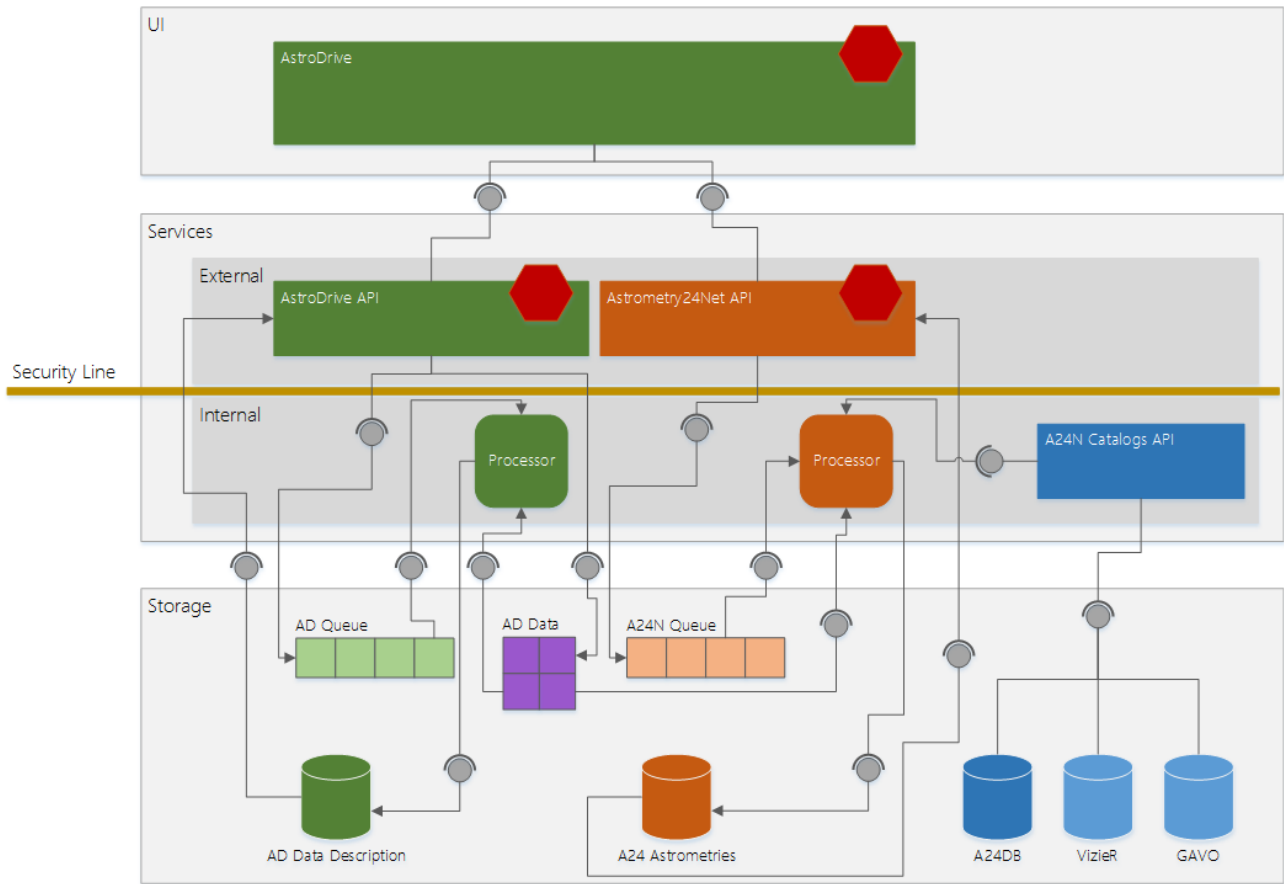


Figure 1 An overall diagram of the system architecture that embeds Astrometry24.NET functionality in a full user-accessible web portal under Sybilla Technologies' AstroDrive (AD), a web service and storage for astronomical images. The conceptual division of the elements within the diagram is emphasized with colours: green – the elements of the AD system, orange and blue – the elements of the Astrometry24.NET (A24N) system that are utilized in AD. The distinction between orange and blue denotes the processing vs. static catalogues' storage. Red hexagons show the externally accessible endpoints that are secured through an authorization and authentication mechanism. These are above the conceptual Security Line presented in yellow. All the resources, services and storages below that line work in a so-called full-trust environment. Where appropriate, connecting lines indicate input dependency with arrows.

The A24N tool is intended as a response to all of the above. It is an online, cloud-based service offering an advanced, user-friendly graphical user interface (GUI), with its own inbuilt astrometric engine, able to recognize streaks as well as point sources and provide an accurate astrometric solution for all extracted features.

Our most important area of improvement, compared to what is currently available on the market, is a tool which, while being (at least) a match in terms of astrometric accuracy to the currently available of-the-shelf tools, is able to perform source extraction and profile fitting of streaks (left by non-sidereal moving objects or stars in the case of non-sidereal tracking) and not only point sources. Beyond that, A24N offers the following improvements over existing tools:

- artificial frames testing to have on-the-fly system accuracy checking,

- cloud storage and manipulation (incl. sharing, searching) of user data,
- advanced online GUI as well as CLI, including batch processing and export of reduction results,
- fully parallel, scalable and N+1 redundancy ready,
- streak profile fitting,
- web based statistics of streaks and point sources.

2 SYSTEM ARCHITECTURE

Astrometry24.NET is a service for an efficient astronomical image astrometric processing with the focus on SST and NEO objects. The architecture for such a system reflects the functional requirements giving space for the performance and usability requirements.

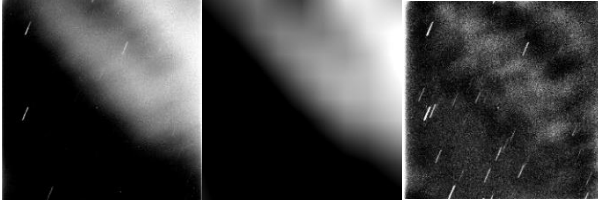


Figure 2: Sample frame obtained with a telescope in a non-sidereal tracking mode (left). Background estimated using the described method (centre). Original frame with the background subtracted (right).

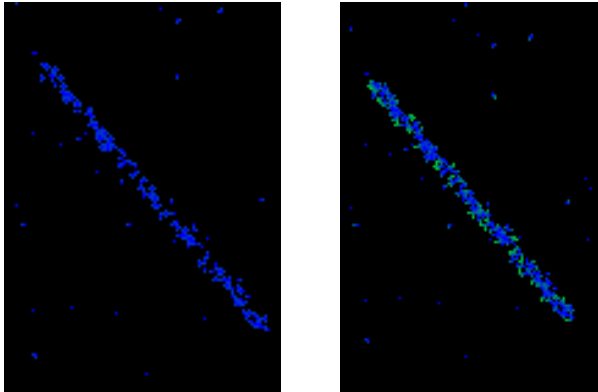


Figure 3: Blob detection hysteresis sample case – before (left) and after (right) applying the hysteresis function.

In Astrometry24.NET the functionality is accessible as a secure web service and within the project it utilizes Sybilla Technologies’ AstroDrive, a web portal/web service for storing astronomical data. This composition allows for a more user-friendly access, manipulation, processing preparation and running than bare web API endpoints would allow for. A general overview of the system that implements and utilizes Astrometry24.NET is presented in Figure 1.

3 ALGORITHMS

Three major steps are required to obtain the astrometric solution of an astronomical image: (1) feature extraction, (2) catalogue star matching and (3) plate solving. A set of specialized algorithms have been designed, implemented and deployed within the Astrometry24.NET service.

3.1 Feature extraction

It is assumed that the input image is an array of 16-bit monochrome pixels. Two types of features are recognized: point sources and extended sources (streaks). They are differentiated by their compactness which is defined by the ratio of the area of the feature to the area of a circle inscribed on the feature.

3.1.1 Frame background

The first step in source extraction is background level estimation and correction, if necessary. Uneven background can have various sources: vicinity of the illuminated Moon, passing clouds lit by artificial lights or reflections of light sources in the optics of the telescope. Uneven background influences the value of the computed background level and increases the value of the standard deviation resulting in an increased value of the threshold. Decreasing the thresholding tolerance may lead to false positive detections of non-existing sources mimicked by high background levels.

The typical approach when dealing with uneven background usually employs some kind of filtering, e.g. median filtering with a large kernel. Although simple, this method suffers from a long computing time and is not well suited for images densely populated with features. Other methods that have been evaluated include high-pass filtering composed of linear average filters, morphological local maxima of local minima of the image. The method that was found to be most effective is a hybrid approach: spline background estimation. It is a combination of spline fitting and median filtering. First, the image is divided into non-overlapping square segments. The typical size of such segment is 100-200 pixels. The median value of all pixels in each segment is computed. The obtained median values are associated with the centre of their corresponding segments creating a grid. Next, a bilinear spline is fitted to the grid. Once the parameters of the spline are computed, the discrete grid obtains an analytical form and a synthetic background is computed for every pixel in the image. This method is fast and works well when applied to frames with uneven background and background gradients – Figure 2.

Once the background fluctuations are removed, the level of the frame’s background is estimated using a histogram of the entire image. The histogram’s peak value is treated as an estimate of the background level. The right slope of the distribution is used to determine the FWHM and σ . These values are then fed into the extraction algorithm.

3.1.2 Image binarization

Creating a binary mask of the image is the last phase before extracting features from the image. Image segmentation is done in two phases: (1) colouring adjacent pixels with labels and creating contiguous regions table in the next step, and (2) extracting contiguous regions from the image – blob detection. Adding a hysteresis function aids in joining features that have no connected pixels but lie close to each other (see Figure 3 for an example). This is especially valuable for low SNR streaks.

3.1.3 Low SNR features

Before binarizing the image, the image can undergo additional filtering, especially if low-SNR features are to be detected. The most efficient method implemented is the Matched Filter which works by applying an oriented kernel to the image. The kernel is a template that is correlated with the original image to enhance similar features. The process of applying this algorithm to a non-sidereal tracking frame is shown in. Figure 4.

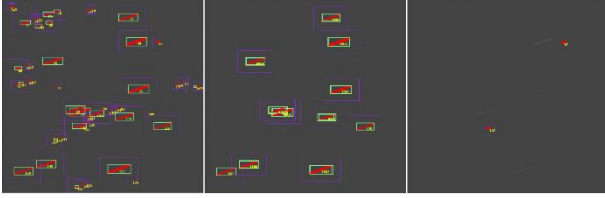


Figure 4: Detection result of Matched Filter Streak Feature Detector (left), extracted streak features for matching (middle), extracted point sources (right).

Image filtering procedures create a modified version of the image with changed shapes of features and modified values of pixels. For example: if a hot pixel is not removed in the first stage, after applying a blur filter its energy is spread across its local neighbourhood resulting in a PSF similar to that of a star. Having this in mind, extracted features have their parameters calculated with respect to real image data.

3.2 Star catalogue matching

The reference plate matching algorithm operates on a set of points, i.e. the detected features need to be represented by the following numbers: centroid coordinates (x, y) , intensity – called plates. The intensity does not need to have a specific unit. It is used only during the sorting process to retrieve the brightest features. For point sources, it is straightforward to use the computed feature characteristics. In the case of streaks, a simple linear fit to the feature's pixels is computed to get a more precise estimate of the centre of the streak and its length. Orthogonal linear regression (total least squares) is used to cope with vertical streaks. In both cases, the same set of numbers is provided to the matching algorithm.

The frame plate is generated from the list of features, while the reference plate is generated from the output of the star catalogue. An estimated frame centre in equatorial coordinates and the pixel scale are required in order to project the star catalogue data to the reference plate. Two projections are implemented: gnomonic and orthographic. Reference stars are selected within a search radius that is 1.5-2.5 times larger than the field of view. The frame plate consists of M brightest features. M is a configurable value between 4 (the minimum number of features required to proceed with the

matching algorithm) and 6. The number of template stars (N) is 15-25 times larger than M and is limited by the catalogue. Objects in both plates are sorted according to decreasing brightness. A vector between the brightest object in both plates is computed and the reference plate is translated so that both stars are now at the same point (pivot point). The reference plate is then rotated by 1 degree around the pivot point. Next, distances between all N and all M features are computed. If a given distance is lower than a predefined value (usually between 10-20 pixels) the two stars may be considered a match. For a given rotation angle a minimum number of star pairs need to be found. Once this condition is satisfied, the exact rotation angle is computed (the iteration loop has a resolution of only 1 degree) and the following iterations are limited to ± 5 degrees from this preferred angle. If the first pivot point does not lead to a solution, the next object from the frame plate is chosen, a new translation vector is computed, and the rotating loop is repeated. Usually it takes no more than a few iterations to match the brightest star from the reference plate with the brightest feature from the frame plate.

3.3 Plate solving

The final step is fitting plate constants to the matched stars. This is performed using least squares methods from the *Alglib* framework³. Assuming that P stars have been matched, a set of $2P$ equations is minimized (x and y for each star-feature pair):

$$\Delta x = \xi - x = a_x \cdot x + b_x \cdot y + c_x + p \cdot x(x + y) + x \cdot (d_1 x^2 + d_2 xy + d_3 y^2) \quad (1)$$

$$\Delta y = \eta - y = b_y \cdot x + a_y \cdot y + c_y + q \cdot y(x + y) + y \cdot (d_1 x^2 + d_2 xy + d_3 y^2), \quad (2)$$

where

$$\xi = \frac{\cos \delta \sin(\alpha - \alpha_0)}{\sin \delta \sin \delta + \cos \delta_0 \cos \delta \cos(\alpha - \alpha_0)},$$

$$\eta = \frac{\cos \delta_0 \sin \delta - \sin \delta_0 \cos \delta \cos(\alpha - \alpha_0)}{\sin \delta \sin \delta + \cos \delta_0 \cos \delta \cos(\alpha - \alpha_0)}$$

are the plate coordinates in the CCD frame (arbitrary units). Δx and Δy are minimized and the following plate constants are obtained: zero point – c_x and c_y , scale – a_x and a_y , rotation – b_x and b_y , plate tilt – p and q , OFAD⁴ – d_1 , d_2 , and d_3 . A sample solution is shown in Figure 5.

³ www.alglib.net

⁴ Optical Field Angle Distortion

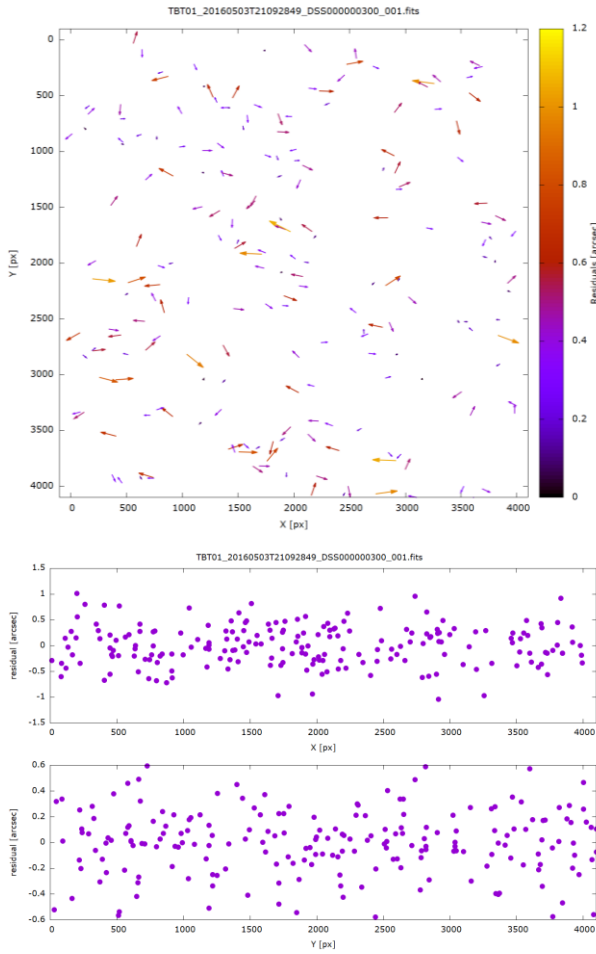


Figure 5: Residuals in frame coordinate space in vector representation (top), X-coordinate (middle) and Y-coordinate (bottom) for a sample TBT frame.

3.4 Configuration

Feature extraction, catalogue matching and plate solving require proper configuration to produce good results. All user-dependent parameters are stored in a configuration file. It is possible to select the preferred algorithm for feature extraction, the plate fitting model and control respective parameters of the algorithms. Usually, one configuration file is sufficient for a given telescope/camera setup and observing strategy combination.

4 WEB PORTAL

The Astrometry24.NET web portal is built on top of AstroDrive, our web application dedicated to management of astronomical observational data, see Figure 6 and Figure 7. The primary goal of the AstroDrive is to mimic cloud storage applications, such as OneDrive or GoogleDrive, and provide tools required

for efficient management and processing of FITS files using the web browser. FITS files are supported natively using our SlimFITS library⁵. The application is developed using the Aurelia framework 1.x+⁶, and it is written in Typescript 2.5+⁷. Being built as a web application, it ensures maximum cross-environment compatibility. The primary support is focused on the Chrome browser (Windows, MacOS, Linux), however, all WebKit-compatible browsers should also work (such as Safari on MacOS/iOS). Access to the portal is governed by OAuth2 authorization (token-based), using ST-IdentityServer⁸.

The portal functionality is split into three areas: file management, file import/processing and single file view/process. The core functionalities include:

- displaying basic file/folder information: name, modification/creation date, size, sharing, processing status and type,
- sorting files/folders: by name, date, modification/creation date and size (both ascending and descending), with option to keep folders on top,
- selecting files/folders: single or multiple selection is supported, along with basic keyboard bindings, such as shift+click, ctrl+click, cmd+click, ctrl+a, cmd+a. Select all icon is also available in the list view,
- performing actions on selected items, depending on a number of selected items: if one item is selected, the toolbar shows its actions, if multiple items are selected, the toolbar shows possible actions for the selection, if no item is selected, the toolbar shows the current folder actions. It is possible to selected both files and folders, in such a case, the toolbar will show *Share* and *Delete* actions,
- basic filtering: by file/folder name,
- Double click to navigate to the item.

The user is able to switch between list and tile view, with no loss of the functionality. Last user settings are remembered between browser sessions (HTML5 Local Storage is used).

⁵ <https://github.com/sybilla/slimfits>

⁶ <http://aurelia.io>

⁷ <https://www.typescriptlang.org>

⁸ <https://github.com/IdentityServer>

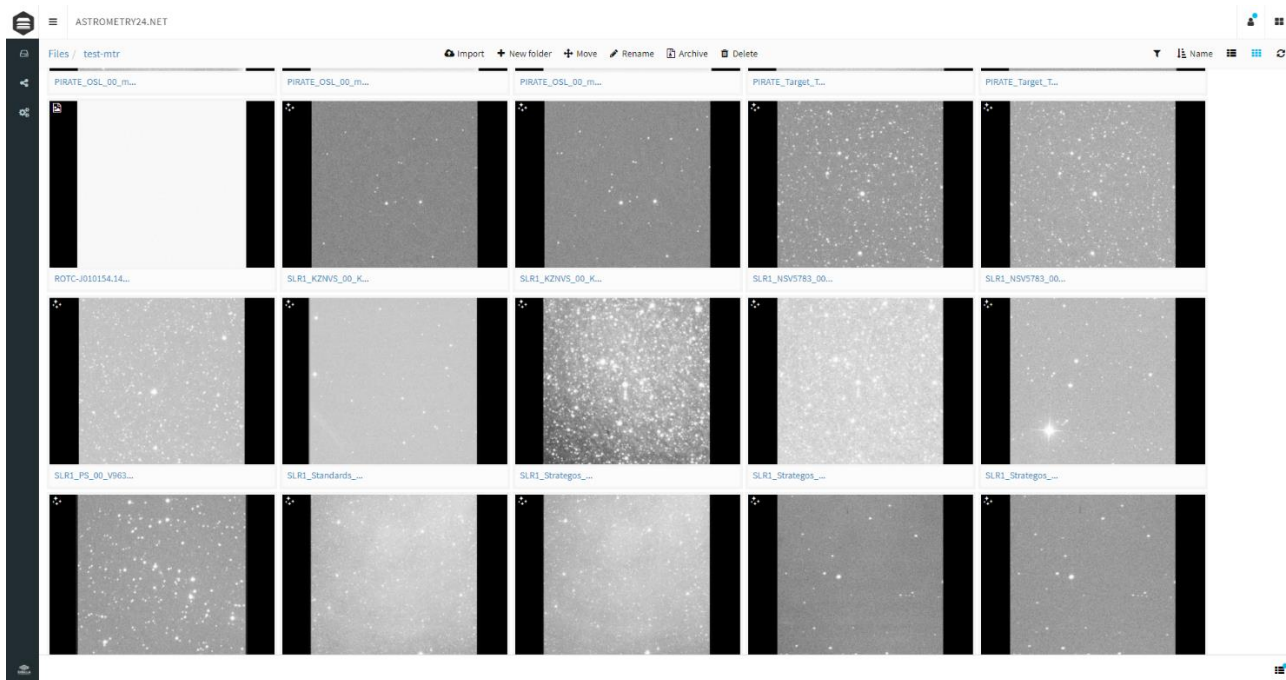


Figure 6: A24N portal, tile view.

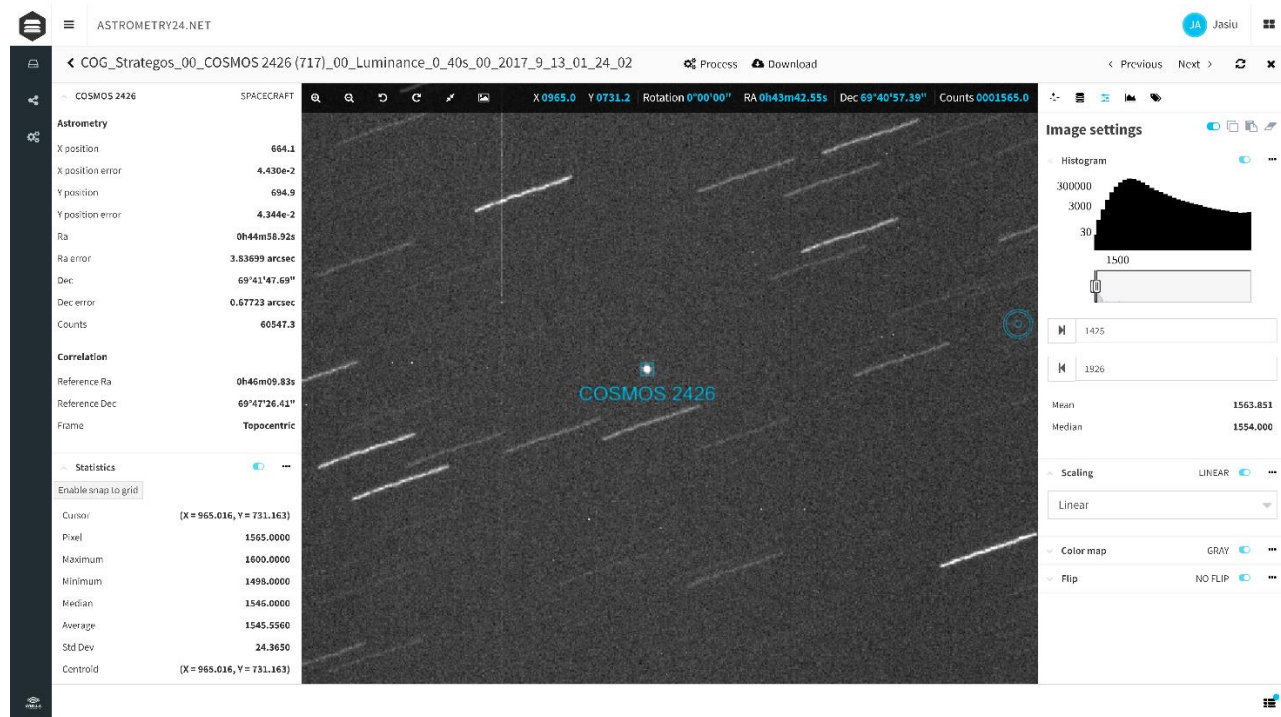


Figure 7: A24N portal, single file view. Selected object data and cursor statistics shown on the left sidebar, image settings (histogram, scaling, colour map, flip, mean and median of the image) on the right sidebar.

5 TESTS

The comparison of Astrometry24.NET and Astrometry.net is presented in Table 1 for a set of 130 OGS frames. The achieved effectiveness and accuracy of both tools are comparable.

Table 1: Comparison of A24N and Astrometry.net test results from a real data set.

METRIC	A24N	Astrometry.net
Total number of frames	130	130
Solved frames	130	129
Solved frames [%]	100%	99.23%
Max RMS ["]	3.04	6.70
Min RMS ["]	0.08	0.16
Median RMS ["]	0.21	0.91

A summary of the test results using synthetic data is presented in Table 2. A total of 99 frames have been generated with a background level of 6000 and $\sigma = 60$ with OGS-based parameters (pixel scale 0.69384 "/px, binning 2x) starting at RA = 01:01:54 and DEC = -66:34:14 and sky-scanning with a step of 0.2 degrees in RA and DEC. Dense fields were avoided (separation of objects larger than 10 pixels), as well as fields with very bright object which would saturate quickly.

Table 2: Comparison of A24N and Astrometry.net test results from synthetic data set.

METRIC	A24N	Astrometry.net
Total number of frames	99	99
Solved frames	99	91
Solved frames	100.00%	91.92%
Max distance of frame centres ["]	4.43E-02	1.61E+00
Min distance of frame centres ["]	5.58E-04	5.87E-02
Median distance of frame centres ["]	1.12E-02	2.05E-01

The final test was conducted only with A24N as it involved streak detection and their measurements. The synthetic data always contained three streaks of various length, position and brightness (peak intensity between 6000 and 24000), aligned along the same angle. The overview of the results is shown in Table 3.

Table 3: Comparison of A24N streak detection with the ground truth data from synthetic frame generator.

METRIC	A24N
Total number of frames	99
Solved frames	99
Solved frames	100.00%
Max RMS ["]	0.19
Min RMS ["]	0.03
Median RMS ["]	0.09
Number of streaks in the frame	3
Number of found streaks	373
Number of correct identifications	278
Percent of correct identifications	74.53%
Number of false identifications	95
Percent of false identifications	25.47%
Min distance for streaks centres ["]	0.01
Max distance for streaks centres ["]	42.52
Median distance for streaks centres ["]	0.16

The comparison of A24N results with precise SP3 solutions for NEO objects confirmed subpixel precision and accuracy on real data (see Figure 9 for an example).

6 OBSERVING CAMPAIGN

6.1 Geostationary satellite monitoring

To test the algorithms and architecture in the production environment we have selected ASTRA 19.2°E satellites. ASTRA is a constellation of 16 geostationary communication satellites, with the 19.2°E group broadcasting to over a 100 million households in Europe [2]. ASTRA has earlier been used in an ESA SST programme experimental tracking campaign [3].

Our campaign was carried out in Jan 2019 with the Panoptes-COG sensor in Garching, Germany (for details on the sensor see e.g. [4]). The ASTRA 19.2°E group consists of four satellites: 1KR, 1L, 1M and 1N.

Figure 8 shows an example frame and the locations of tracks obtained for all four 19.2°E group member objects. These are shown individually in a close-up in Figure 10 – Figure 13 .

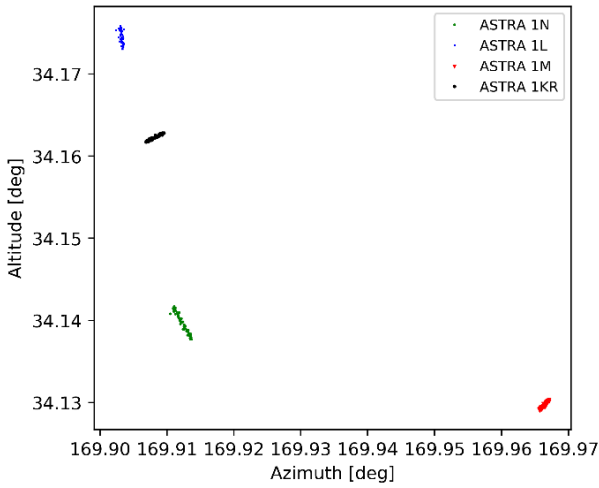
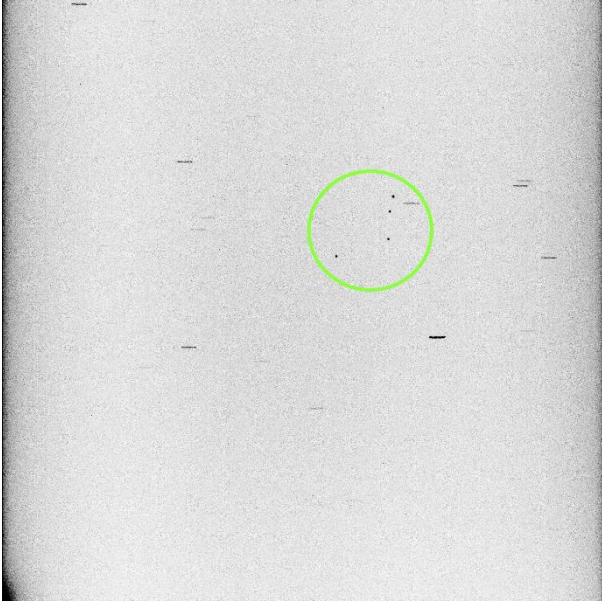


Figure 8. ASTRA 19.2°E group of satellites observed with COG. Top: example frame with the four satellites marked with the green circle. Bottom: alt-az plot of all observation points.

The observations were performed in an object-tracking mode. The observed trend (data points forming lines) is expected and is due to the so-called longitude drift and, associated with it, orbital station-keeping. The alt-az plots show straight-line fits to the data points together with rms values derived for those fits. The bottom panel in each figure shows altitude change as a function of Modified Julian Date (MJD).

The obtained preliminary rms values are 0.041, 4.765, 0.374, and 2.213 arcsec for ASTRA 1KR, 1L, 1M, and 1N, respectively. The 1KR and 1M values are very good, well within 1 arcsec rms; the values for 1L and 1N are affected by the visible outliers and the final result will clearly improve with further data reduction.

6.2 Navigation satellite monitoring

Long term monitoring of the COG sensor accuracy, precision and offset has been conducted on BeiDou IGSO 5, Cosmos 2425, 2426, 2477, 2501, and PRN 05, 07, 24, and 26 navigation satellites.

BeiDou is the Chinese navigation satellite system⁹, with 33 operational satellites as of November 2018, of which six (including the observed IGSO5) are in the 55-deg inclined geosynchronous orbit (IGSO). The Cosmos satellites are part of the Russian GLONASS navigation satellite system¹⁰, with 24 satellites currently in orbit. PRN satellites form part of the American Global Positioning System¹¹, currently consisting of 31 operational satellites.

In Table 4 we provide observation details and statistics for all the observed satellites. Figure 14, Figure 15 and Table 5 provide detailed example results for the Beidou IGSO5 satellite.

Using the collected data, we performed orbit determination. Our analysis consisted of the following steps:

- computing observation residuals relative to the SP3 reference orbit,
- performing orbit determination using the Kalman filtering method,
- computing position and velocity residuals between the determined and reference SP3 orbit.

Figure 14 shows observation residuals relative to the SP3 reference orbit for IGSO5. The residuals are small, with the uncorrected values' rms of 0.33 ± 0.07 arcsec in declination (DEC) and 1.47 ± 0.07 arcsec in right ascension (RA). Once offset-corrected, the values significantly improve to 0.24 ± 0.06 and 0.29 ± 0.05 .

To perform orbit determination, we used Orekit¹²; see Figure 15 for orbit fitting residuals and Table 5 for residuals of orbit determination relative to the SP3 reference orbit.

The obtained results confirm the suitability of the COG sensor for SST observations.

⁹ <http://en.beidou.gov.cn/>

¹⁰ <https://www.glonass-iac.ru/en/>

¹¹ GPS, <https://www.gps.gov/>

¹² <https://www.orekit.org/>

7 SUMMARY AND CONCLUSIONS

The A24N web service presents an important step in astrometric data processing where the user experience is web based and does not require installation of any third-party software, is always up to date and is easily scalable due to the cloud resources usage. A thin cross-platform client with command line interface is also available for Windows, Linux, and Mac OS. The architecture of the service allows for an easy incorporation of new or existing algorithms and will improve user experience where the same familiar layout may be used for multiple algorithms. A24N provides support tools for the investigation of each astrometric processing step in the web interface as well as image statistics analysis. Our solution provides a unified experience and a smooth transition from an automatic batch setup and processing to a non-standard data investigation.

We have developed algorithms and services that allow for robust astrometry on frames with both sidereal and non-sidereal tracking and both point sources and streaks. The accuracy and precision tested on real and synthetic data shows that the service is already comparable to or better than Astrometry.net or Astrometrica. The performance tests showed that the service can process typical real data frames with the speed of one frame per few seconds, depending on their size. With the cloud computing scaling capability, even the throughput of sCMOS camera producing 100 frames per second will not be an issue for the service and only the constant delay of a few seconds will be introduced between the image acquisition and obtaining an astrometric solution.

As such, A24N has the potential to play an important role in a European, real-time and autonomous network for the detection of hazardous objects orbiting Earth.

ACKNOWLEDGEMENTS

A24N has been developed for ESA by Sybilla Technologies (prime) and Cilium Engineering (subcontractor) under the contract no. 4000119510/17/D/SR.

We thank the staff of the Mt. Suhora Observatory of the

Pedagogical University in Kraków, Poland, Nicolaus Copernicus Astronomical Centre of the Polish Academy of Sciences, Poland, the School of Physical Sciences of The Open University, UK, and the Astronomical and Geophysical Observatory of the Comenius University, Slovakia, for making available the test data used in the earlier stages of A24N development.

REFERENCES

- [1] „Space Debris: the ESA Approach,” [Online]. Available: http://download.esa.int/esoc/downloads/BR-336_Space_Debris_WEB.pdf.
- [2] E. Bertin i S. Arnouts, „SExtractorL Software for source extraction,” tom 117, pp. 393-404, 1996.
- [3] D. Lang, D. W. Hogg, K. Mierle, M. Blanton i S. Roweis, „Astrometry.net: Blind Astrometric Calibration of Arbitrary Astronomical Images,” *The Astronomical Journal*, tom 139, nr 5, pp. 1782-1800, 2010.
- [4] „Very Low Cost Satellite Interactive Services - SES-Astra,” [Online]. Available: <https://artes.esa.int/projects/very-low-cost-satellite-interactive-services-ses-astra>.
- [5] „Satellite Tracking Campaign Tests European Abilities,” [Online]. Available: https://www.esa.int/Our_Activities/Operations/Space_Situational_Awareness/Satellite_tracking_campaign_tests_European_abilities.
- [6] M. Konacki, P. Lejba, P. Sybilski, R. Pawłaszczek, S. Kozłowski, T. Suchodolski, M. Litwicki, U. Kolb, V. Burwitz, J. Baader, P. Groot, S. Bloemen, M. Ratajczak, K. Helminiak, R. Borek i P. Chodosiewicz, „Polish and European SST Assets: the Solaris-Panoptes Global Network of Robotic Telescopes and the Borowiec Satellite Laser Ranging System,” w *Proceedings of the Advanced Maui Optical and Space Surveillance Technologies Conference*, Wailea, Maui, Hawaii, 2016.

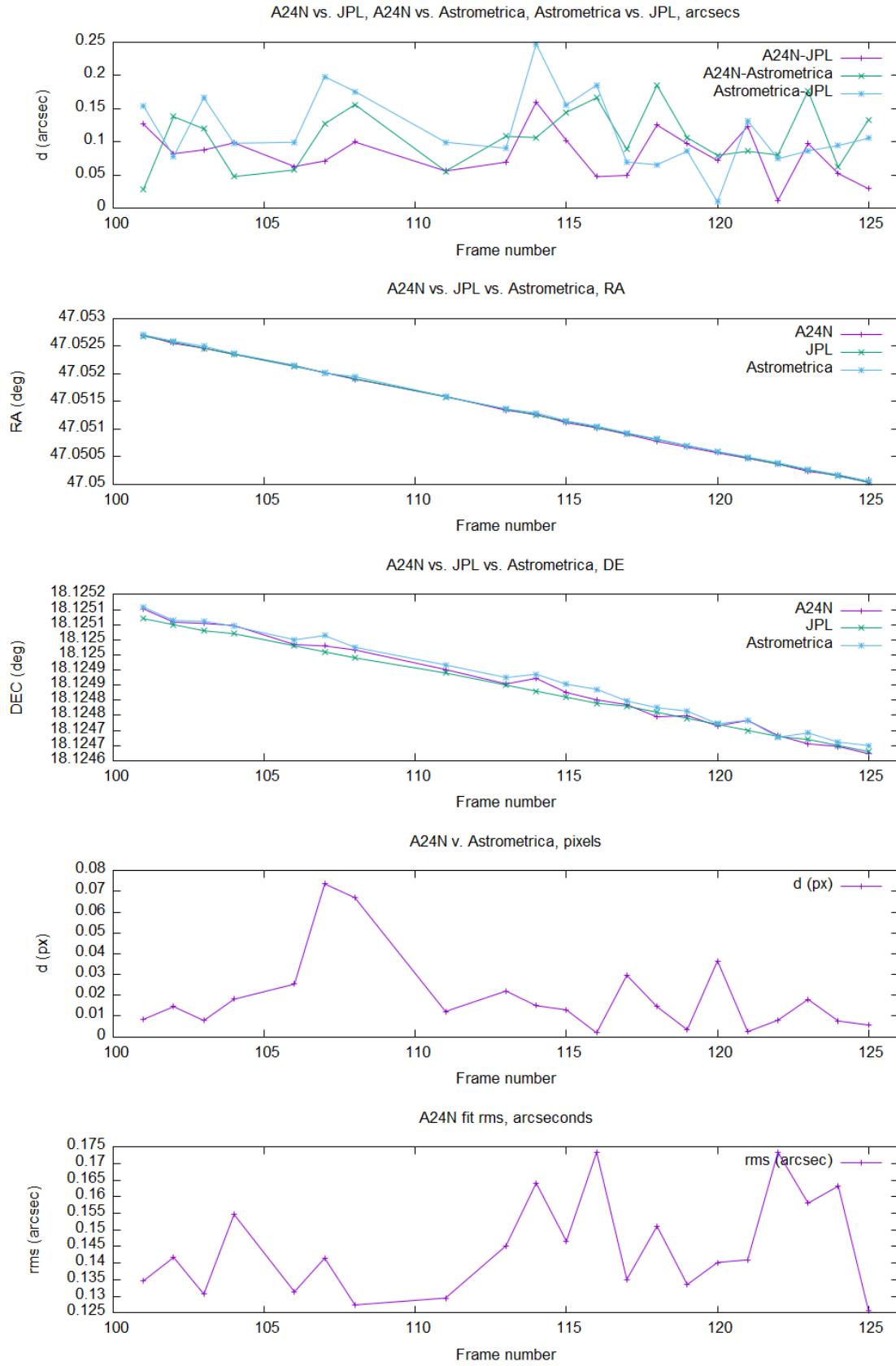


Figure 9: Comparison of NEO astrometry for asteroid 09642. Average SNR of the object of interest is 79. Accuracy and precision better than 0.2 pixel are achieved when compared with JPL and Astrometrica.

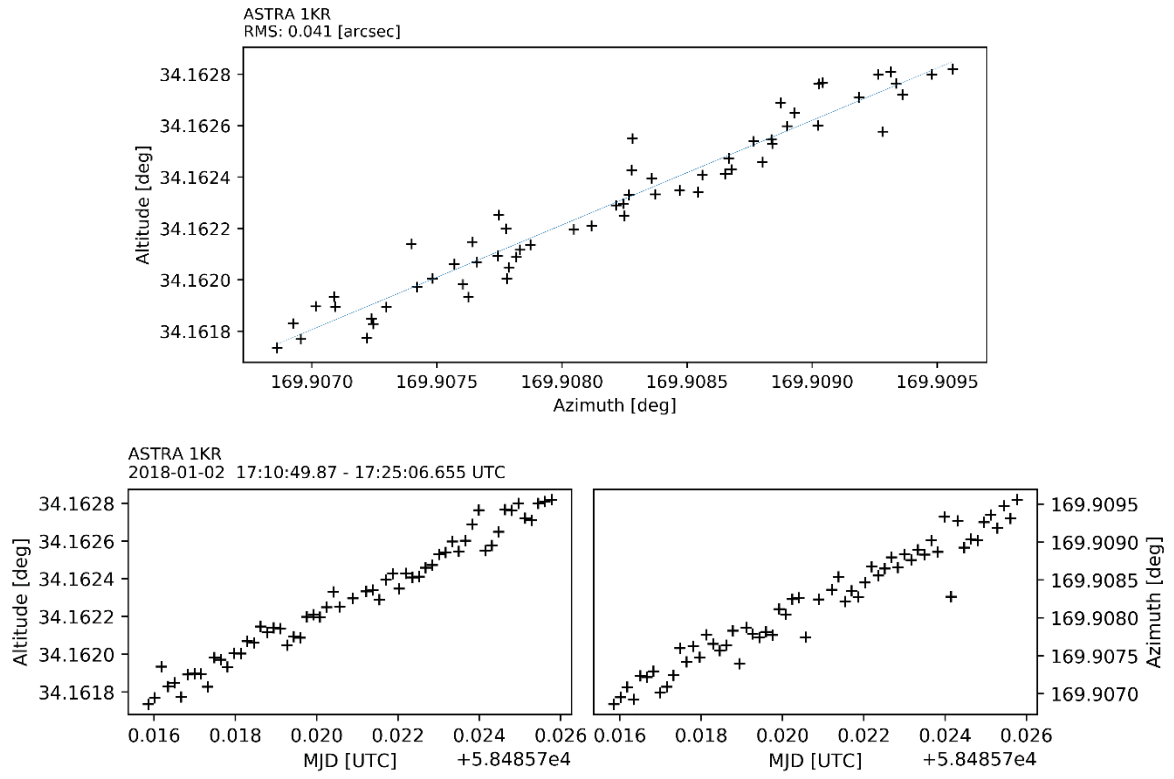


Figure 10. ASTRA 1KR. Top: alt-az plot with a straight-line fit and rms value around it quoted in the top, left-hand corner of the figure. Bottom: altitude (left) and azimuth (right) as a function of MJD.

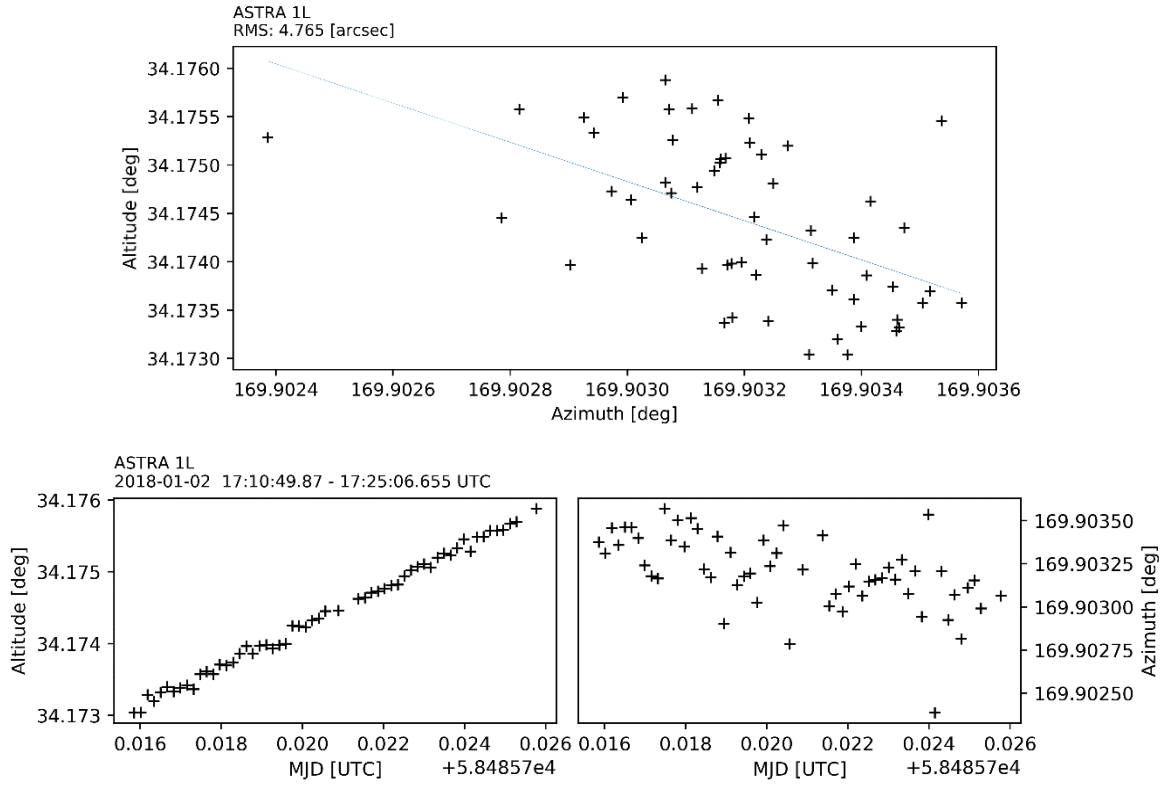


Figure 11. As in Figure 10 but for ASTRA 1L.

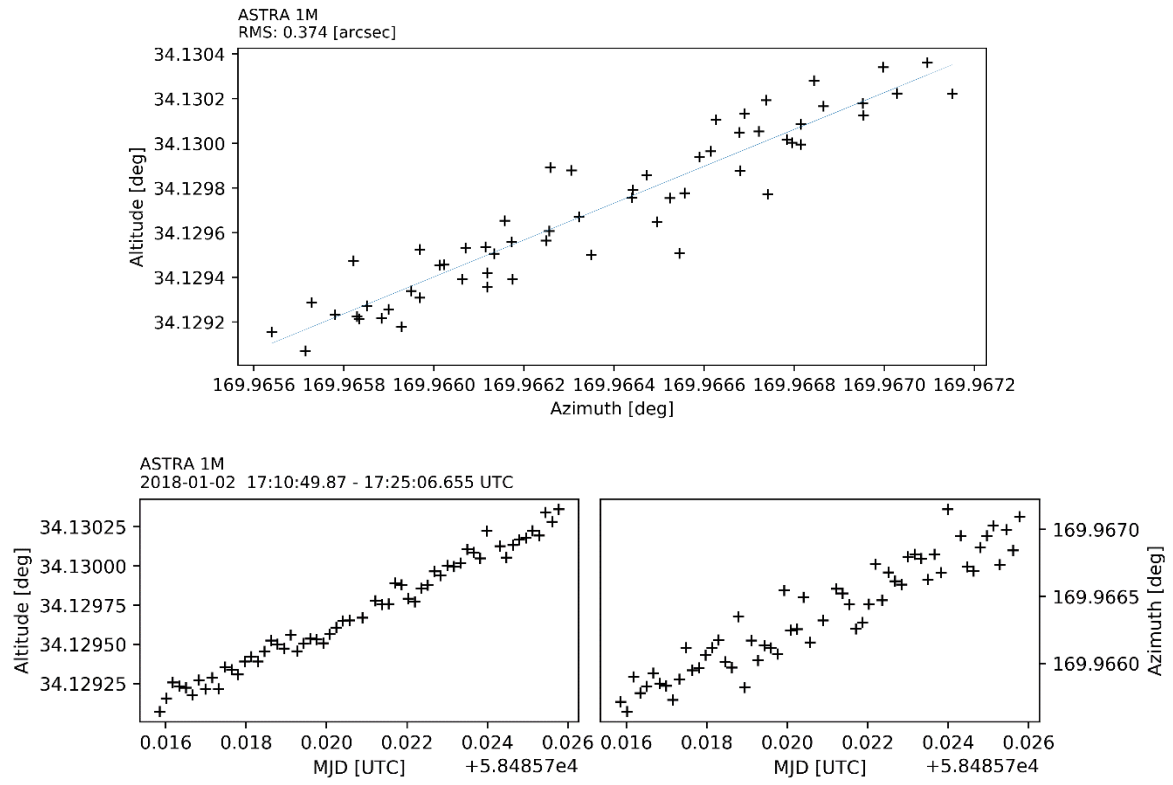


Figure 12. As in Figure 10 but for ASTRA 1M.

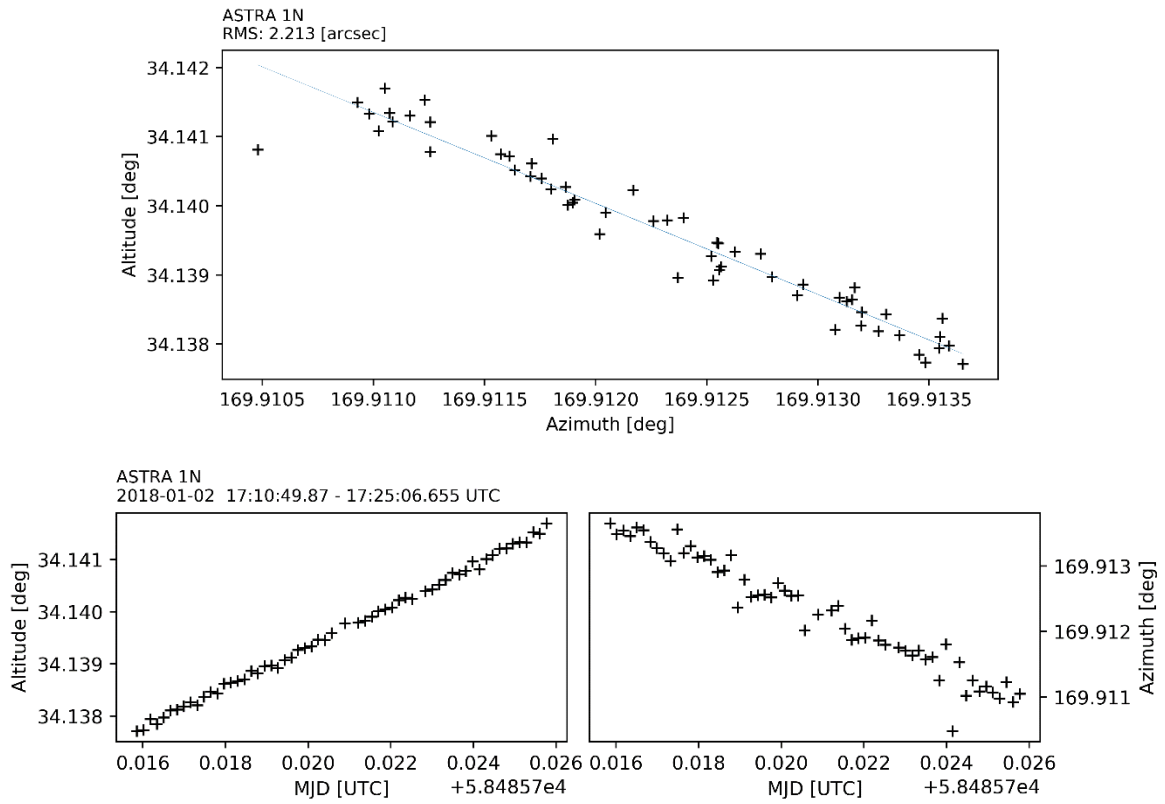


Figure 13. As in Figure 10 but for ASTRA 1N.

Table 4. Data processing statistics and results for the COG telescope validation campaign.

	Satellite	Observation date	Time interval	Number of single frames	RMS raw [arcsec]		RMS corrected [arcsec]	
					RA	DEC	RA	DEC
1	IGSO5	2018-10-04	20:12 - 20:41	122	1.4682	0.4097	0.3359	0.2177
2		2018-10-05	19:10 - 19:39	123	1.4195	0.2744	0.2273	0.1566
3		2018-10-09	19:32 - 20:01	126	1.4941	0.4063	0.2707	0.2959
4		2018-10-10	19:00 - 19:59	251	1.4666	0.3593	0.2574	0.2991
5		2018-10-15	17:25 - 19:20	229	1.4855	0.2543	0.3004	0.2456
6		2018-10-17	18:16 - 18:45	125	1.3927	0.2624	0.3674	0.2468
7		2018-10-18	18:44 - 19:14	126	1.4209	0.2761	0.2136	0.1478
8		2018-10-21	19:09 - 19:38	126	1.6133	0.3942	0.33	0.2963
9	PRN 05	2018-10-15	19:21 - 19:49	213	0.963	0.4211	0.2564	0.421
10		2018-10-18	17:45 - 18:14	202	1.1169	0.705	1.0377	0.6905
11		2018-10-25	19:22 - 19:31	57	1.0912	0.4221	0.3734	0.4189
12	PRN 07	2018-10-03	20:15 - 20:38	139	1.2878	0.8977	0.7097	0.786
13		2018-10-05	18:12 - 20:09	341	1.0797	0.5382	0.5077	0.504
14		2018-10-07	18:06 - 18:35	175	0.7985	0.2589	0.2795	0.2549
15		2018-10-15	17:50 - 18:19	212	0.9379	0.1835	0.3078	0.1803
16		2018-10-19	17:43 - 19:30	321	1.1111	0.5648	0.5705	0.5546
17		2018-10-20	18:11 - 18:34	102	1.281	0.8194	1.0057	0.8008
18	PRN 24	2018-10-19	00:54 - 22:56	112	0.823	0.4604	0.3906	0.4215
19	PRN 26	2018-10-18	02:44 - 03:57	397	1.1691	0.3733	0.4398	0.3681
20	COSMOS 2425	2018-10-15	20:20 - 20:49	210	0.8807	0.8355	0.4942	0.7011
21		2018-10-19	03:05 - 03:54	97	0.8472	0.5642	0.5012	0.5507
22	COSMOS 2426	2018-10-19	18:12 - 18:42	205	1.0161	0.5875	0.5811	0.5872
23	COSMOS 2476	2018-10-05	20:10 - 21:09	352	1.109	0.7202	0.3715	0.7202
24		2018-10-21	17:40 - 19:08	387	0.7894	0.3915	0.2466	0.3873
25	COSMOS 2477	2018-10-06	00:58 - 01:18	122	1.4286	0.8361	0.8073	0.8283
26		2018-10-17	17:21 - 17:46	180	0.6586	0.3358	0.6262	0.3233
27		2018-10-18	17:20 - 17:44	176	1.1203	0.6119	0.3012	0.6057
28	COSMOS 2501	2018-10-10	18:00 - 18:29	210	0.7109	0.2636	0.4268	0.2537
29		2018-10-17	18:46 - 19:16	209	0.4507	0.2742	0.2517	0.2627
30		2018-10-18	18:15 - 18:44	212	0.8788	0.4252	0.5415	0.4154

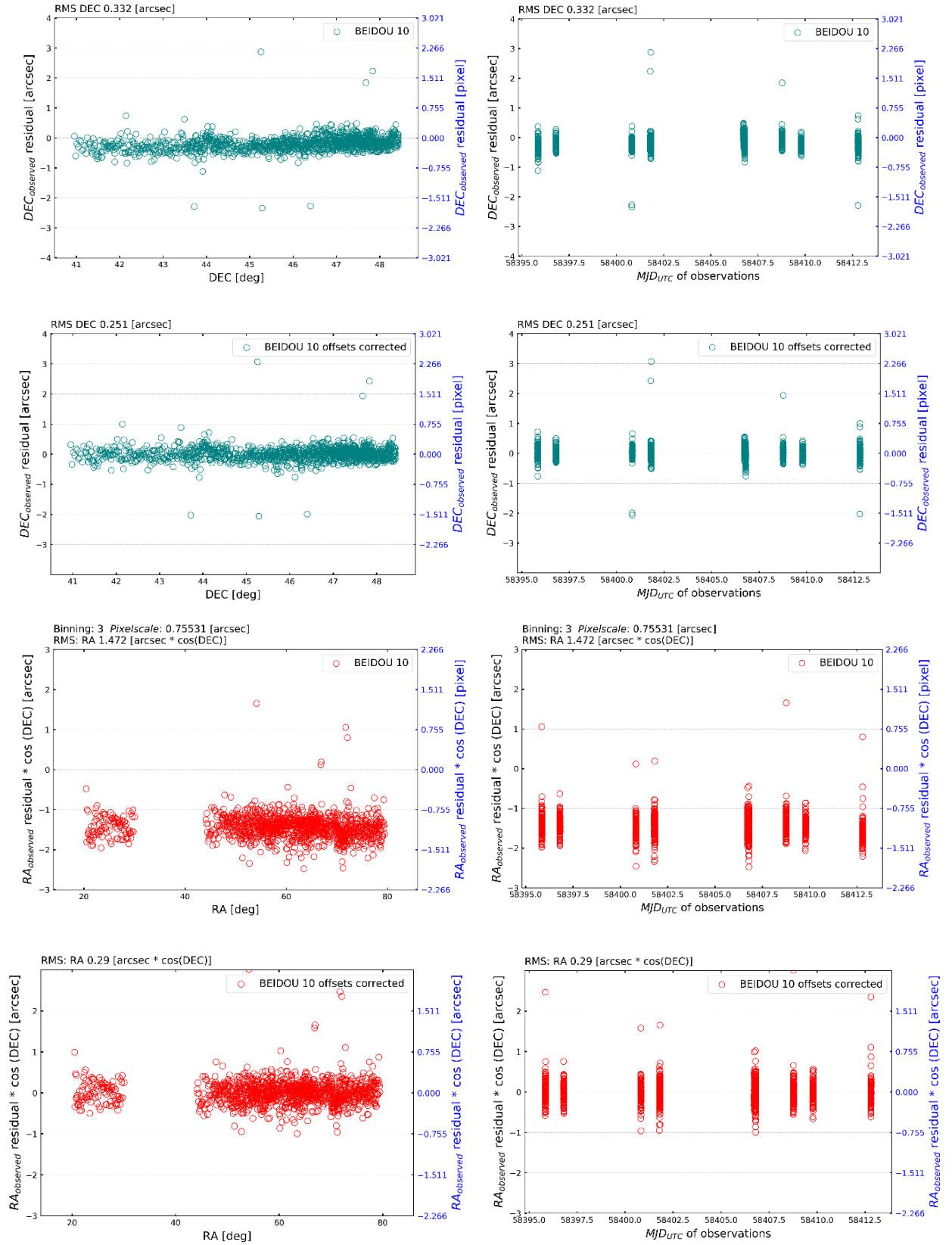


Figure 14. Observation residuals relative to the SP3 reference orbit for the BeiDou constellation member - IGS05 (here denoted as BeiDou-10) satellite. DEC (uncorrected in row 1 and offset-corrected in row 2) and RA (as for DEC but rows 3 and 4, respectively) residuals vs. reference DEC/RA values (left column) and vs. MJD (right column).

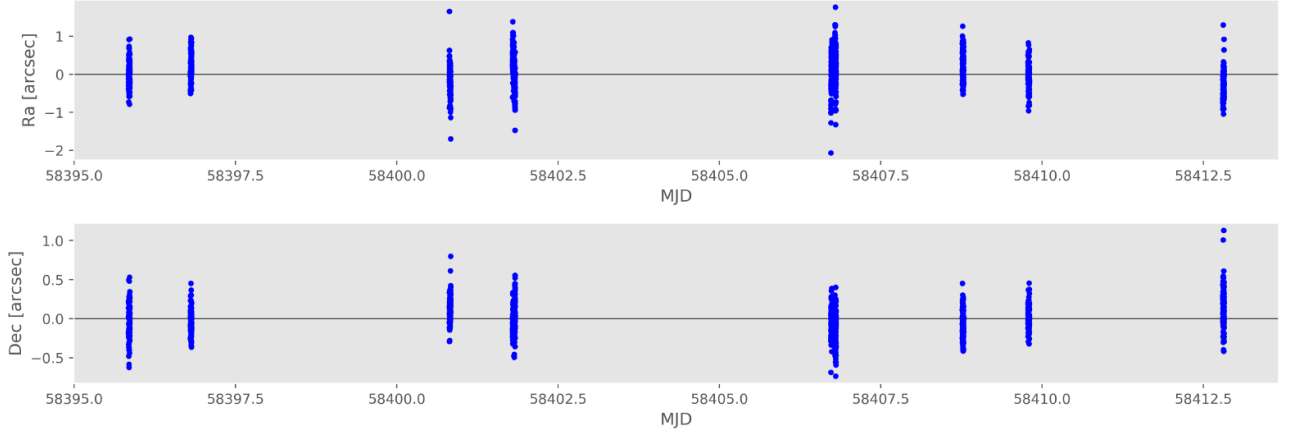


Figure 15. BeiDou constellation IGSO5 satellite: orbit fitting residuals (top: RA, bottom: DEC).

Table 5. BeiDou constellation IGSO5 satellite: residuals of orbit determination relative to the reference SP3 orbit (back propagated using Kalman filtering). (1) observation date and time window, (2) number of individual frames included in the analysis (whose absolute *o-c* values are <99.7 percentile; cf. Table 4 for the total number of frames), (3)-(5) average radial, along track and cross track residuals, (6)-(8) rms values for the radial, along track and cross track residuals, (9) total rms value.

Date&Time	#obs	\bar{R}_r	\bar{R}_v	\bar{R}_x	<i>rms</i> R_r	<i>rms</i> R_v	<i>rms</i> R_x	<i>rms</i> R
2018-10-04 20:00 : 21:00	120	118.85	262.83	239.68	118.9	263.15	239.93	375.441
2018-10-05 19:00 : 20:00	123	138.36	215.6	177.81	138.38	215.62	177.87	311.899
2018-10-09 19:00 : 21:00	124	115.84	217.3	199.15	115.9	217.52	199.39	317.022
2018-10-10 19:00 : 20:00	249	119.11	206.49	185.01	119.29	206.9	185.77	302.571
2018-10-15 17:00 : 20:00	229	128.68	225.45	173.15	129.7	229.78	173.4	315.733
2018-10-17 18:00 : 19:00	124	121.47	182.66	148.9	121.49	182.72	148.93	265.195
2018-10-18 18:00 : 20:00	126	109.8	186.39	170.82	109.86	186.53	171.05	275.897
2018-10-21 19:00 : 20:00	125	96.83	233.42	213.94	96.84	233.87	214.27	331.639